Title
Functional Morphology of Sea Otter (Enhydra lutris spp.) Forelimbs with Respect to Tool-Use

Author
Hupka, Brandon Dean

Publication Date
2018

Peer reviewed|Thesis/dissertation

UNIVERSITY OF CALIFORNIA

Los Angeles

Functional Morphology of Sea Otter (*Enhydra lutris spp*.) Forelimbs with Respect to Tool-Use

A thesis submitted in partial satisfaction

of the requirements for the degree Master of Science

in Biology

by

Brandon Dean Hupka

2018

ABSTRACT OF THE THESIS

Functional Morphology of Sea Otter (*Enhydra lutris spp*.) Forelimbs

with Respect to Tool-Use

by

Brandon Dean Hupka

Master of Science in Biology

University of California, Los Angeles, 2018

Professor Blaire Van Valkenburgh, Chair

The superfamily Musteloidea represents an ecologically and morphologically diverse collection of mammals. Lutrinae, the subfamily within Musteloidea that contains otters, includes 13 extant species across five continents in a variety of (semi-)aquatic/marine environments. Besides elucidating musculature, skeletal structures can provide evidence for behavior and ecology. In this study, we use linear measurements and 2-dimensional geometric morphometric analysis of the three forelimb long-bones (humerus, radius, and ulna) from eight species of extant otters, as well as a number of subspecies, to observe whether unique tool-use behavior of sea otters can be analytically captured and differentiated from other otters.

The thesis of Brandon Dean Hupka is approved.

David K. Jacobs

Michael E. Alfaro

Blaire Van Valkenburgh, Committee Chair

University of California, Los Angeles

2018

Dedicated to the shoulders I stand on.

TABLE OF CONTENTS

LIST OF FIGURES

INTRODUCTION:

The sea otter, *Enhydra lutris*, is the smallest of the marine mammal carnivores but the largest in body mass of the living otters. *Enhydra* was historically distributed along the Pacific Rim from the northern Japanese island of Hokkaido, north to Russia (primarily the Kamchatka Peninsula and Sea of Okhotsk), eastward across the Bering Strait and across the southern margin of Alaska, and continued south along the North American coast as far as Baja California (Kenyon 1969). The fur trade, which began in the 18th century and ended in the early 20th century, decimated sea otter populations and consequently served to create discontinuity in their distribution and limit it substantially. It is estimated that the historical population of sea otters worldwide was several hundred thousand to one million (Kenyon 1969). Following the enactment of the Treaty for the Preservation of Fur Seals in 1911 by Japan, Russia, Great Britain, and the United States, the sea otter received some protection in the form of a harvesting moratorium. In subsequent years, the otter received more governmental protection, and consequently their numbers and distributions have since recovered somewhat (Kenyon 1969). At present, there are estimated to be approximately 100,000 sea otters in the wild in a discontinuous and disintegrated distribution, although the IUCN erroneously lists the population as being not severely fragmented (Doroff and Burdin 2015). Despite the historical population bottleneck, theoretical and empirical data suggest significant genetic diversity was not lost either in small populations or across the whole species (Cronin 1996).

While sea otters are not unique among Lutrinae with regards to the time spent in the water, they are unique in how they forage and feed in neritic aquatic environments. Sea otters are known to eat fish and other non-benthic prey, but are best known for using hard objects, primarily rocks, as

anvils to aid in retrieving near-offshore benthic invertebrate prey from their hard shells (Kenyon 1969). Sea otters dive for prey and use their sensitive, furless palms and digits to feel for and retrieve benthic invertebrates from rocks. They then surface, float on their backs, and place a rock or hard shell, also often retrieved from the ocean floor, on their ventral side and use it as an anvil. Holding the prey between their forepaws, they raise their forelimbs above their head, and repeatedly strike the prey against the anvil. After consuming the meat of the prey, sea otters will often clean themselves of the exoskeleton and then continue foraging (Kenyon 1969). It is imperative that they meticulously clean their pelage so as to retain its buoyancy and insulative properties (Estes 1980). Occasionally, sea otters will stow the tool in a pocket of loose axillary skin and reuse it for the next feeding event (Kenyon 1969).

The two primary goals of this study are to determine whether sea otters have specialized forelimb morphologies that are attributable to their unique tool-use among Lutrinae, and to determine whether there are differences among the three subspecies of sea otter with regards to tool-use frequency or magnitude of strength required for tool-use. Forelimb morphology is quantified in all three subspecies of sea otter as well as seven other otter species, all of which do not use tools (*Aonyx capensis, Aonyx cinereus, Hydrictis maculicollis, Lontra canadensis, Lontra felina, Lontra longicaudis,* and *Pteronura brasiliensis*).

The three subspecies of sea otter vary in tool-use frequency (Fujii et al. 2015). The California sea otter (*Enhydra lutris nereis*) uses tools at a high frequency, but the Southeast Alaska subspecies (*E. l. kenyoni*) and the Aleutian Islands subspecies (*E. l. lutris*) use tools less frequently. Data are particularly insufficient for *E. l. lutris,* but Fujii et al. (2015) observed that more eastern (with

respect to the Pacific Rim) populations tend to use tools more often. Alaskan otters presented with clams that were too difficult for them to open with their teeth or paws alone (clams that they would be unlikely to happen upon in their natural habitat) struck the clams against a rock or another clam against their chest. Kenyon referred to this phenomenon as a "frustration behavior," but did not acknowledge it as an explicit and deliberate use of tools (Kenyon 1969). This suggests that sea otters are capable of tool-use whether they frequently use tools or not, and suggests that they elect to use tools only when absolutely necessary. Not all California sea otters use tools, nor do individuals necessarily use tools at the same frequencies (Fujii et al. 2015). Feeding preference is adopted matrilineally, and it is postulated that variable feeding preferences among rafts of sea otters might minimize feeding competition and food stress among close relatives (Estes et al. 2003).

Despite variation in the frequency of tool-use among sea otters, we hypothesized that their forelimb skeleton would differ from that of non-tool using otter species. In particular, we predict that the forelimb bones (humerus, radius, and ulna) of sea otters will exhibit features that enhance mobility at the elbow and wrist, as well as strength and mechanical advantage of muscles such as the triceps and deltoids that are involved in the hammering of hard prey. In addition, within *Enhydra*, we predict that the California subspecies (*E. l. nereis*) will exhibit these features to a greater degree than the other two subspecies. To test this, we use traditional morphometric methods such as linear measurements as well as geometric morphometrics to capture shape differences. In addition to exploring differences among otter species and *Enhydra* subspecies, we tested for differences between modern and pre-fur trade midden-pile California

sea otter bones. The modern to midden comparison was done to explore possible historical shifts in sea otter behavior.

METHODS:

Twenty linear measurements of the humerus, radius and ulna were taken of *n* adults of each otter species and the three sea otter subspecies (Table 1). Linear measurements were adapted from Meachen-Samuels and Van Valkenburgh (2009), and are described in Table 2. The measurements were used to construct a set of functional ratios or indices (Table 3). In addition to measurements, digital images of the bones in lateral and medial views were recorded for each bone. Each limb bone was positioned similarly for imaging.

Midden pile specimens from the Santa Barbara Museum of Natural History consisted exclusively of sea otters from San Miguel Island, California, and date from as old as the early Holocene (Braje 2007). These specimens are included only in the analysis of linear measurements of individual bones and not geometric morphometrics.

Prior to 1991, sea otters found north of California and east of Eurasia were referred to as *E. l. lutris*, but in 1991, Wilson et al. assigned all these otters to *E. l. kenyoni*. When measuring specimens, we assigned them to subspecies according to their provenance rather than the museum classification because many specimens were collected prior to 1991 and have not since been updated.

STATISTICAL ANALYSES AND LANDMARKS:

Linear measurements were log transformed and then analyzed in R. We use packages "curl," "devtools," "ggplot2," "Rcpp," and "ggbiplot" accessed through Github in order to acquire the software necessary for analyzation. Principal component analyses (PCA) were run on humerus, radius, and ulna measurements, as well as a combined dataset including all three bones. Non-graphical summary statistics were also generated in the R console. Ratio graphs were generated using the "ggplot" package.

A geometric mean size proxy was calculated for each of the specimens by taking the third root of the product of the total lengths of each of the long bones (humerus, radius, and ulna). Sea otter midden specimens were assigned geometric mean values imputed from available data. Samples of each bone were chosen randomly and added together to simulate one tripled specimen, such that each solitary specimen was randomly assigned two more long bones.

In order to analyze the photographs, the "PointPicker" plugin for ImageJ/Fiji was used. Landmarks were selected for each of the three bones and images of these landmarks can be seen in the Appendix (Figures 6A, 7A, 8A). These data were collected and used in MorphoJ for 2-dimensional morphometric analysis.

In order to analyze our photographic data, we used MorphoJ to first generate a Procrustes fit and then generated a covariance matrix from the ImageJ geometric morphometric data. Executing these analyses in MorphoJ allowed us to run a PCA and generate a PC1/PC2 graph (Appendix, Figures 6C, 7C, 8C). The eigenvalues and loadings generated from this analysis allowed us to

determine the most important PC scores and can be found in the Appendix. Landmark graphs that depict "lollipops" designating where most of the variation is, can be found in the Appendix (Figures 6B, 7B, 8B). Data for all analyses can be found in the Appendix.

Designated landmarks for the humerus can be seen in the Appendix (Appendix, Figure 6A). Landmarks 1H, 2H, and 3H were chosen because they outline the corners of the deltoid crest. The deltoid muscle is of particular interest for us because of its role in brachial abduction and general brachial stabilization. These aspects are crucial in sea otter tool-use. Landmark 4H is placed at the most proximal point of origin of the extensor carpi radialis longus, a muscle that controls abduction of the hand at the wrist (Howard 1973). This landmark might elucidate usage or robusticity of the extensor carpi radialis longus. It is known that sea otters use their forepaws together to grasp prey and tools, due to their lack of digital dexterity, and thus rely on wrist dexterity (Kenyon 1969). Landmark 5H was placed on the lateral epicondyle and is important in conjunction with Landmark 1H in providing a measure of length. It should be noted that these landmarks were additionally chosen due to their quality of being consistently identifiable across all specimens.

Designated landmarks for the radius can be seen in the Appendix (Appendix, Figure 7A). Landmarks 1R and 2R mark the proximal width of the radius, while 5R and 6R mark the distal width of the radius. With these landmarks, we hope to capture information on robusticity and articulation. Landmarks 3R and 4R mark the proximal edge and distal edge of the biceps tuberosity, respectively. The biceps tuberosity might reveal important information about mechanical advantage of the antebrachium as well as the importance of the biceps brachialis.

Designated landmarks for the ulna can be seen in the Appendix (Appendix, Figure 8A). Landmarks 1U and 2U mark the most proximal ends of the olecranon process. 1U marks the anteriormost corner of the olecranon process and 2U marks the posterior apex of the olecranon process. These landmarks were chosen because they identify prominent aspects of the proximal ulna and can be consistently identified. Landmark 3U marks the most proximal and prominent end of the trochlear notch while landmark 4U marks the most anterior and prominent end of the coronoid process. These landmarks delineate the width of the trochlear notch and provide information about distance from 1U and 2U, which would elucidate mechanical advantage of the triceps muscle, as well as articulation with the humerus. Landmark 5U, which sits between the styloid process and distal head of the ulna, was primarily chosen for its ease of identification and use in providing a length dimension to the ulna data.

RESULTS:

LINEAR MEASUREMENTS:

Humerus. Principal component analysis (PCA) on the six humeral measurements resulted in PC1 explaining 94.6% of observed variation, and PC2 explaining 3.3% of observed variation (Figure 1). Otter species are separated primarily along PC1 by body size, with smaller otters such as *A. cinereus* (ACI*)* and *L. felina* (LFE) having positive values and and larger otters such as *Pteronura* and *Enhydra* having negative values. On PC2, *Enhydra* separates from other species and has more positive values especially relative to the similar sized *Pteronura*. It should be noted that while the humeri of *Pteronura* and *Enhydra* are similar in length, *Enhydra* is a heavier animal. The variable that appears to be most responsible for this separation is HDAP, the

anteoposterior compression of the distal articular surface at the trochlear notch. *Enhydra* is characterized by a relatively deeply spooled trochlea relative to other otter species. Within *Enhydra*, there is weak separation among the subspecies, with *E. lutris nereis* (ELUn, ELUnM, modern and midden specimens) tending to have smaller HDAP measurements than either their Alaskan or Asian counterparts (ELUk, ELUl). The unusual morphology of the California sea otter is highlighted in a bivariate plot of HDAP against humeral length (HL) (Appendix, Figure

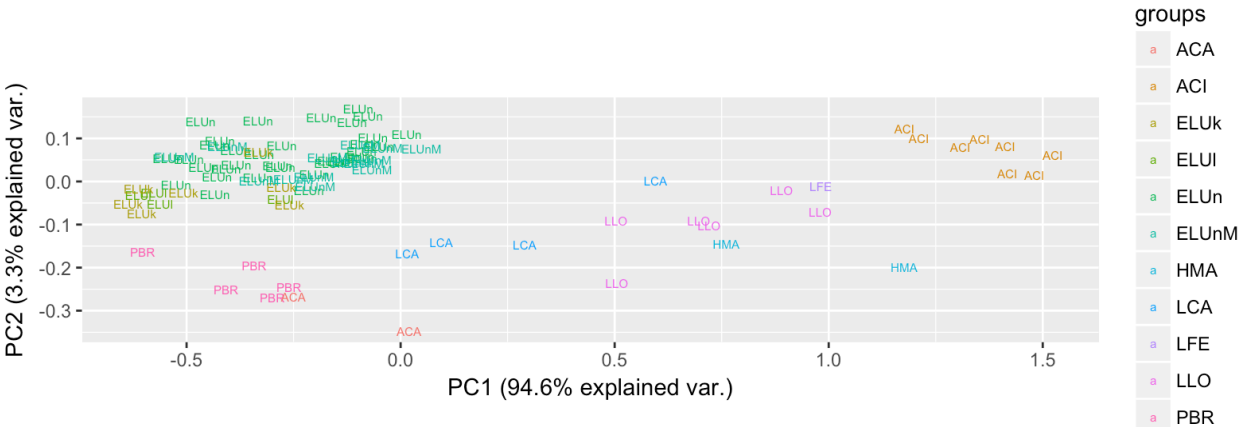

Figure 1, Plot of the first two principal components of the humerus:
Enhydra spp. plot more positively than *Pteronura*, despite being similar in length. *Enhydra* are most separated from other otters on the PC2 axis by HDAP. *E. lutris nereis* tends to plot more positively than other *Enhydra* specimens on both PC axes.

9). California sea otters plot almost exclusively below all other otters and have relatively small HDAPs for their HLs when compared to other sea otter specimens as well as other otter species. In contrast, *Pteronura* and *A. capensis* have very large HDAP/HL ratios.

Radius. PCA on the nine radial measurements resulted in PC1 explaining 92.6% of observed variation, and PC2 explaining 4.2% of observed variation (Figure 2). Otter species are again primarily separated along PC1 by size, with smaller species tending to have more positive values and larger species tending to have more negative values. On PC2, *Enhydra* has more positive values and is separated from *Pteronura*. The variables most heavily loaded on PC2 are the

diameter of the shaft of the radius (RD) and the distance from the radial head to the distal end of the bicipital tuberosity which marks the insertion of m. biceps (RBF). *Enhydra* has a somewhat narrow, elongate radius compared with *Pteronura* despite similar body mass, as can be clearly seen in a bivariate plot of RD against RL (Appendix, Figure 11). Interestingly, *A. capensis* plots

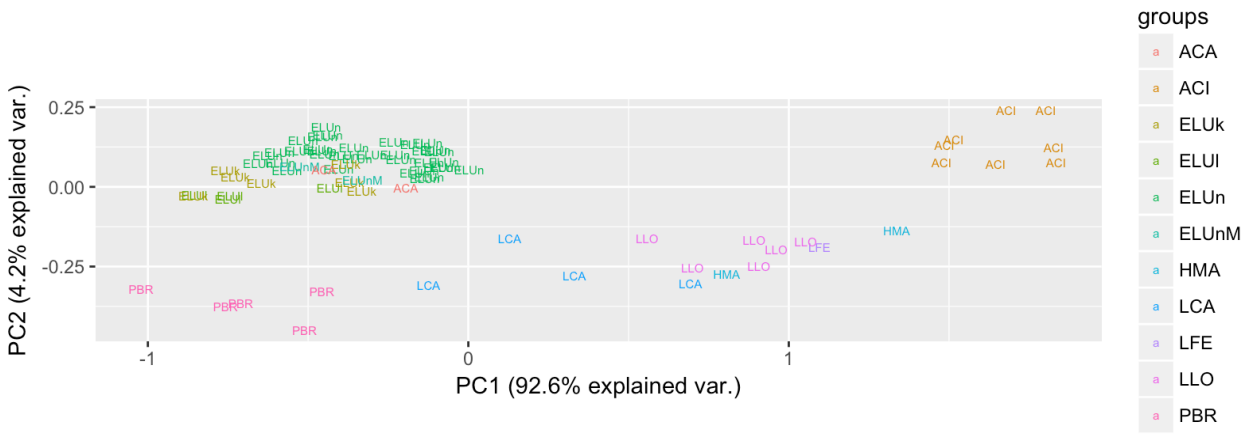

Figure 2, Plot of the first two principal components of the radius:
Enhydra and *Aonyx capensis* plot together and are most distinct from other otters on the PC2 axis by their RD and RBF measurements. *Enhydra* subspecies tend to group together, and California midden specimens, while more negative along the PC2 axis than modern California otters, group most closely with them.

close to *Enhydra* and also has an elongate radius that is much less robust than that of *Pteroneura*. *Enhydra* and *A. capensis* are also similar in having slightly greater RBF than *Pteronura* which could suggest increased mechanical advantage of the biceps muscle. However, the ratio of RBF to RL, which is a proxy for the relative mechanical advantage of the biceps in flexing the elbow, does not differ significantly among the three taxa. Within *Enhydra,* there is considerable overlap, but the California subspecies (ELUn) tends to have slightly more positive values on PC2 and slightly more negative values on PC1 than the other two subspecies.

Ulna. As in the previous linear measurement analyses, otter species are primarily separated along PC1 by size, with smaller otters having more positive values and large otters having more

negative values. However, the ulna varies much more in shape among otter species than either the humerus or radius, as evidenced by PC2 explaining much more of the observed variation, 29.7% as opposed to less than 5% in the humerus and radius analyses (Figure 3). Much of the spread on PC2 is due to the more positive values observed in California sea otter. The most heavily loaded variables on PC2 are the mediolateral breadth of the radial articular surface measured at the coronoid process (UCP) and to a lesser degree, total ulnar length (UL). Unlike

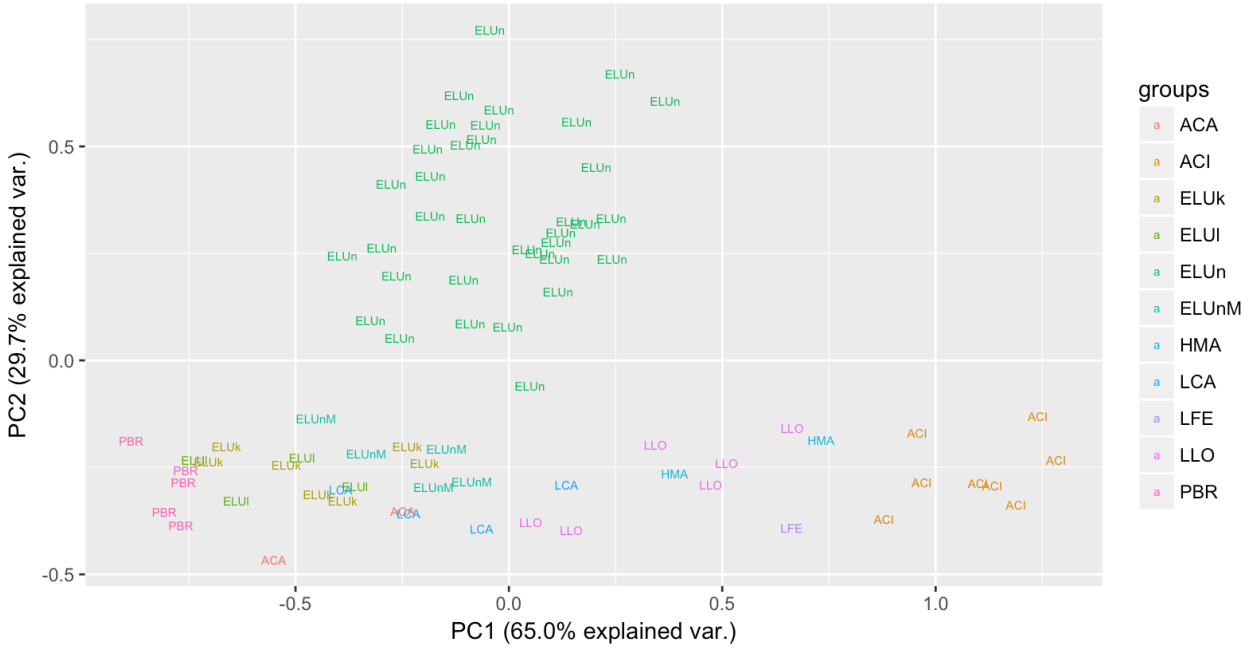

Figure 3, Plot of the first two principal components of the ulna:
California sea otters' uniquely small UCP measurements distinctly separate them from all other otters, including all other *Enhydra* specimens. The California sea otter morphospace displays considerable variability within the subspecies.

in the analyses of the humeri or radii, the three *Enhydra* do not cluster together; instead, the California subspecies has much more positive values on PC2 (albeit with considerable scatter) than the other two taxa. This separation is driven by the much smaller diameter of the radial articulation (UCP) in *E. lutris nereis* than both the other two subspecies and all other otter species.

Brachium & Antebrachium. When the measurements on all three long bones are combined in a single PCA, the distribution of species on PC1 and PC2 is similar to that observed for the plot of the ulna alone (Appendix, Figure 1). PC1 and PC2 explain 83.7% and 11.1% of observed variation, respectively (Figure 4, in Appendix). Otter species are similarly ordered by size across the PC1 axis. On PC2, the California sea otter is well separated from all other taxa and this is largely due to its reduced UCP values. In addition, *Pteronura* is separated from all three *Enhydra* subspecies in having more negative values on PC2, which probably reflects its relatively large olecranon process (ULO).

Brachium & Antebrachium of only *Enhydra*. Looking exclusively at the combined measurements of all three long bones of *Enhydra* in a single PCA, separation of the California sea otter from the other two subspecies is apparent (Figure 5). PC1 and PC2 explain 70.2% and 20.7% of observed variation, respectively, and otters are primarily ordered along both axes by UCP measurements. Otters are secondarily ordered by the anteroposterior depth of the processus anconeus (UPA) along the PC2 axis. On average, California sea otters have smaller UCP and UPA values than other otters, as is apparent in bivariate plots of each of these variables against ulna length (Appendix, Figure 12).

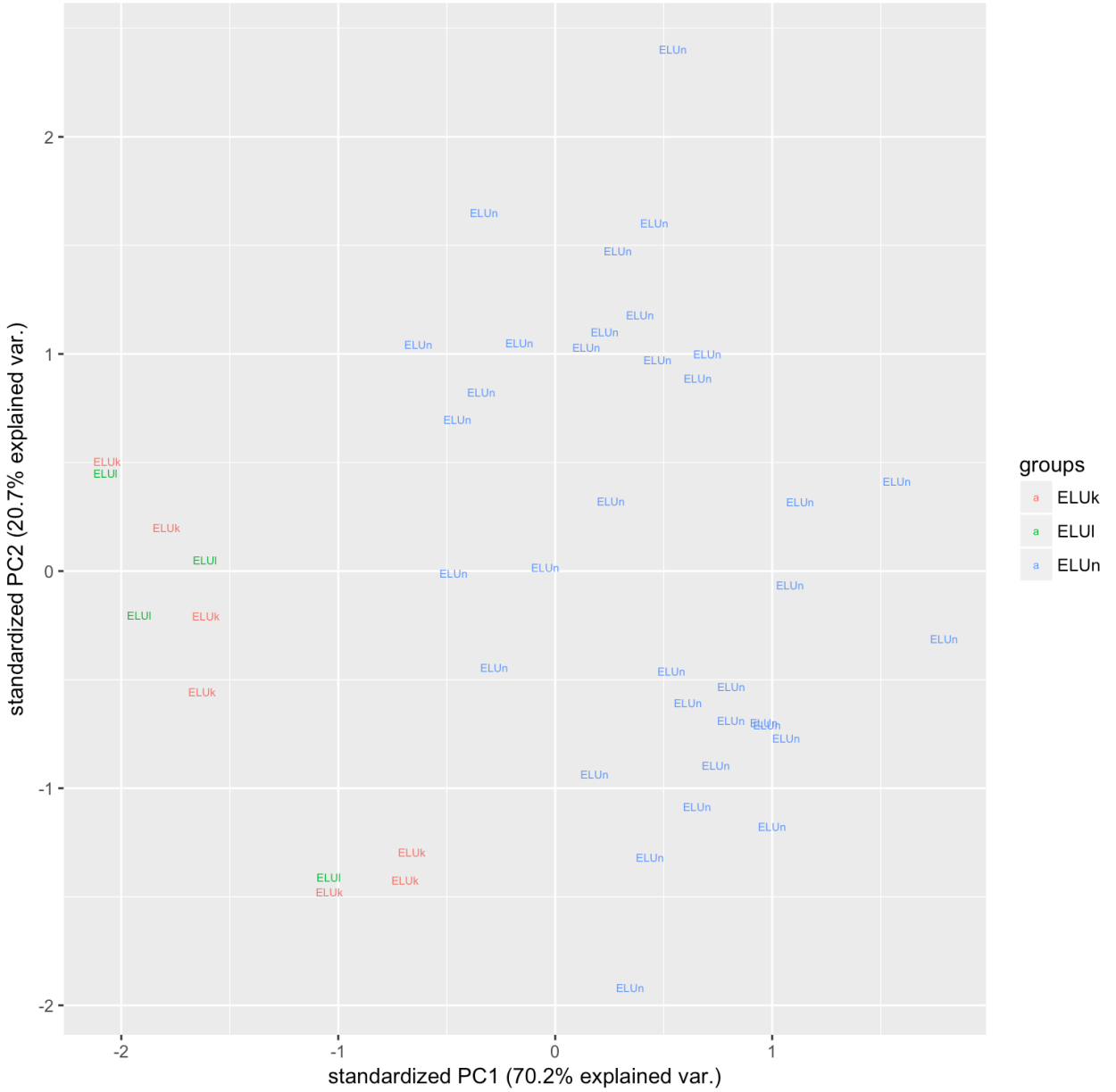

Figure 5, Plot of the first two principal components of the three forelimb long bones of *Enhydra spp*.: California sea otters most separate from Asian and Alaskan sea otters by their small UCP and UPA measurements.

2-DIMENSIONAL GEOMETRIC MORPHOMETRIC ANALYSIS:

Humerus. PCA on the humeral landmark data resulted in PC1 explaining 68.32% of observed variation and PC2 explaining 13.67% (Appendix, Figure 6). Because geometric morphometric

analysis eliminates the need to correct for size and instead focuses on shape differences, PC1 does not order otters by size. Otter species are separated along PC1 by shape variation. Most shape variation is observed in landmarks 3H and 4H, which represent the distal tip of the deltoid crest and origination point for the extensor carpi radialis longus, respectively. Otters with more positive PC1 values have a relatively small distance between landmarks 3H and 4H. Otters with more positive PC2 values have a relatively small distance between landmarks 3H and 4H and landmark 5H. Consequently, otters that have more negative PC2 values tend to have more curved humeri than otters, such as *Lontra canadensis* and *Pteronura brasiliensis*. *Enhydra* clusters separately from other otters on both axes, and is characterized by having relatively larger deltoid crests and more proximal origination points for the extensor carpi radialis longus than other otters. There does not appear to be clear separation of the subspecies within *Enhydra*.

Radius. PCA on the radial landmark data resulted in PC1 explaining 45.20% of observed variation and PC2 explaining 25.41% (Appendix, Figure 7). Most shape variation is observed at the distal end of the radius (landmarks 5R and 6R), however considerable variation is also observed at the proximal end of the radius (landmarks 1R and 2R). On PC1, *Pteronura* has negative values due to its having a broad distal end relative to its proximal head and its overall robusticity. *Enhydra*, while robust, has a radius of more uniforms width, hence it has positive values on PC1. Otter species with less robust, thinner radii, such as *Aonyx sp*. plot more positively along the PC2 axis.

Ulna. PCA on the ulnar landmark data resulted in PC1 explaining 76.16% of observed variation and PC2 explaining 11.25% (Appendix, Figure 8). Most shape variation is observed at landmarks

2U and 4U, which represent the proximal tip of the olecranon process and the tip of the coronoid process, respectively. Otter species with rounded, less robust olecranons, such as *Enhydra* and *Aonyx* plot more negatively along the PC1 axis, whereas species with squared olecranons, such as *Hydrictis* and *Pteronura*, plot positively on PC1. Otter species with more proximal semilunar notches relative to the total length of the ulna place more negatively along PC2, however it should be noted, that overall length can be quite intraspecifically variable based on individual variation of olecranon length (ULO) (Appendix, Figure 13). There is considerable variation in ulnar shape among the three *Enhydra* subspecies. However, California sea otters tend to place more negatively than other sea otter subspecies, indicating that their olecranons are relatively short and favor speed of elbow extension rather than strength. By contrast, *Pteronura* has a robust and long olecranon relative to total ulnar length, and plots more positively on PC2, suggesting adaptation for strength rather than speed.

DISCUSSION:

The forelimb bones of *Enhydra* do differ significantly is shape from those of other otters. Among the humeral measurements, *Enhydra* separates from other otters most with regards to HDAP, or the anteroposterior compression of the distal articular surface at the trochlear notch. *Enhydra* is unique in that, while large-bodied, it has a relatively small average HDAP measurement. This trait might be attributed to the fact that a smaller HDAP may confer a greater amount of stabilization in elbow articulation, which is beneficial to an animal that must use its forelimbs for tool manipulation, particularly in the manner in which the sea otter does. It should be noted that sea otters do not use their forelimbs for swimming and spend less time on land than almost all other otters, and therefore do not require robust bones to support their weight (Tarasoff

et al. 1972). Humerus shape is similar among the three subspecies of *Enhydra* although California sea otters appear to have the narrowest trochlea. The geometric morphometric analysis of the humerus suggests that the deltoid muscles are relatively larger in *Enhydra* than other otters, suggesting adaptation for enhanced strength when flexing the shoulder joint. In addition, the origination point for the extensor carpi radialis longus is more proximal in *Enhydra* relative to other otters, indicating greater strength in wrist extension.

Given the similarity in size between *Enhydra* and *Pteroneura*, it is remarkable that *Enhydra* has such a slender radius for its length as shown by both the geometric morphometric and linear measurement analyses. This likely reflects the fact that, unlike the giant river otter, sea otters rarely walk or run on land and therefore do not need the support of a robust radius. Interestingly *Enhydra* and *A. capensis* are similar in having relatively slender radii for their length and a more distal placement of the bicipital tuberosity. In the case of *Enhydra,* the elongate, slim radius provides a greater speed and range of flexion and extension at the elbow joint. *A. capensis* is a prodigious digger of burrows in riverbanks (Larivière 2001) and perhaps the elongate radius enhances their reach while digging but it is unclear why they do not exhibit more typical skeletal adaptations for digging, such as robust bones and foreshortened antebrachium to enhance strength.

As was true of the radius, the ulnae of *Enhydra* and *Pteronura* occupy discrete morphospaces and display disparate ulnar morphologies (Appendix, Figure 8). *Pteroneura* has a robust, square-shaped olecranon process and a relatively proximal semilunar notch, whereas *Enhydra* specimens have less robust and more rounded olecranons and vary in semilunar notch placement.

This agrees with the findings of Botton-Divet that *Enhydra* has a "slender and curved ulna" (2016). The mean length of the olecranon is less than 16% of total ulnar length in *Enhydra* and all other otters except in *Lontra* (21%) and *Pteronura* (25%).

The ulna showed the greatest variation in shape across all otters and within *Enhydra*. In particular, the California sea otter displayed a very narrow articulation for the proximal radius (UCP) relative to radius length in comparison with the other two sea otter subspecies as well as all other otter species. UCP estimates the mediolateral breadth across the coronoid process of the radial notch (UCP) and captures the shape of the articulation between the radius and ulna. In the California sea otter, the radial head is small and circular in shape, allowing for rapid and extensive movement (supination, pronation) of the manus, a feature that likely contributes to manual dexterity. The absolute size of UCP in California sea otters was similar to that of *A. cinereus*, a much smaller species with an ulna half the length of that of *Enhydra* (Larivière 2003). The UCP of *E. l. nereis* is uniquely small among sea otters, including the three California midden specimens, suggesting this feature may relate to more frequent tool use behavior in extant *E. l. nereis* than more ancient populations.

The forelimb morphology we observed in extant California sea otters might reflect post-fur trade adaptations to altered prey communities. Sea otter populations were decimated as a result of the fur trade and because they are keystone species for kelp forest communities, their absence stimulated an ecosystem shift (Steneck et al. 2002). Once California sea otter populations rebounded, the new population either adjusted to the altered ecosystem or retained a morphological feature from a small founding population. It should be noted that large

invertebrates have been in decline due to habitat destruction and overfishing (Jackson et al. 2001). It is possible that greater radial rotational freedom is needed to adequately forage in the relatively prey-depauperate modern ecosystems where *E. l. nereis* is found. The *E. l. nereis* morphospace is large, indicating substantial variation within the subspecies. Because sea otters do not have identical food preferences to one another and because food preference and hunting strategies are adopted matrilineally, it is possible that this morphospace captures variable feeding methods (Estes et al. 2003). Because diets vary, not all California sea otters use tools, and not all that use tools do so at the same frequency. Given limited food, individuals might benefit by specializing on different prey.

It is clear that *Enhydra*'s unique tool-use behavior is associated with a unique forelimb morphology. Moreover, the subspecies known to use tools most often, *E. l. nereis* is differs from its more northerly cousins, *E. l. kenyoni* and *E. l. lutris*, and even its ancestors from the midden samples of San Miguel Island. This last difference perhaps highlights an adaptation to an altered ecosystem, a founder effect, or, to some extent, both. When sea otters are transplanted from one location where hard-shelled prey are depauperate to another where they are not, individuals will begin striking prey items if necessary (Kenyon 1969). However, it is unclear whether this is a learned, allelomimetic behavior, or an innate one. The apparently unique morphology and behavior of the California sea otter might favor the conservation of each of the three *Enhydra spp*. as separate populations. It is clear that there is phenotypic variation among *Enhydra spp*., however it is unclear how much is genotypic and how much is epigenetic. Post-fur trade founder effects may have shifted the California sea otter from its historic morphology (with respect to the midden specimens analyzed in this study); however it is possible that our midden specimens

represent a “Southern/Baja California” sea otter subspecies that was driven to extinction and historically differed from the central and northern California sea otters that still exist today.

Future studies should further analyze midden specimens, especially in other locales, and other pre-fur trade otters to better understand how morphologies may have since shifted, as well as address if this shift was driven by a founder effect, a shift in prey abundance or ecosystem health, filling an ecological niche left by a now extinct resource competitor, or some combination thereof. Genetic testing of extant sea otters to discover underlying genomic explanations for tool-use and associated morphological features should be undertaken. In terms of morphological studies, it would be of interest to study how the limb bones of sea otters, in particular California sea otters, handle the forces of tool-use (perhaps through Finite Element Analysis), whether they have an enhanced range of forelimb motion, and if the unique morphological traits of California sea otters observed in this study are in agreement with those findings.

APPENDIX:
FIGURES 4, 6-13:

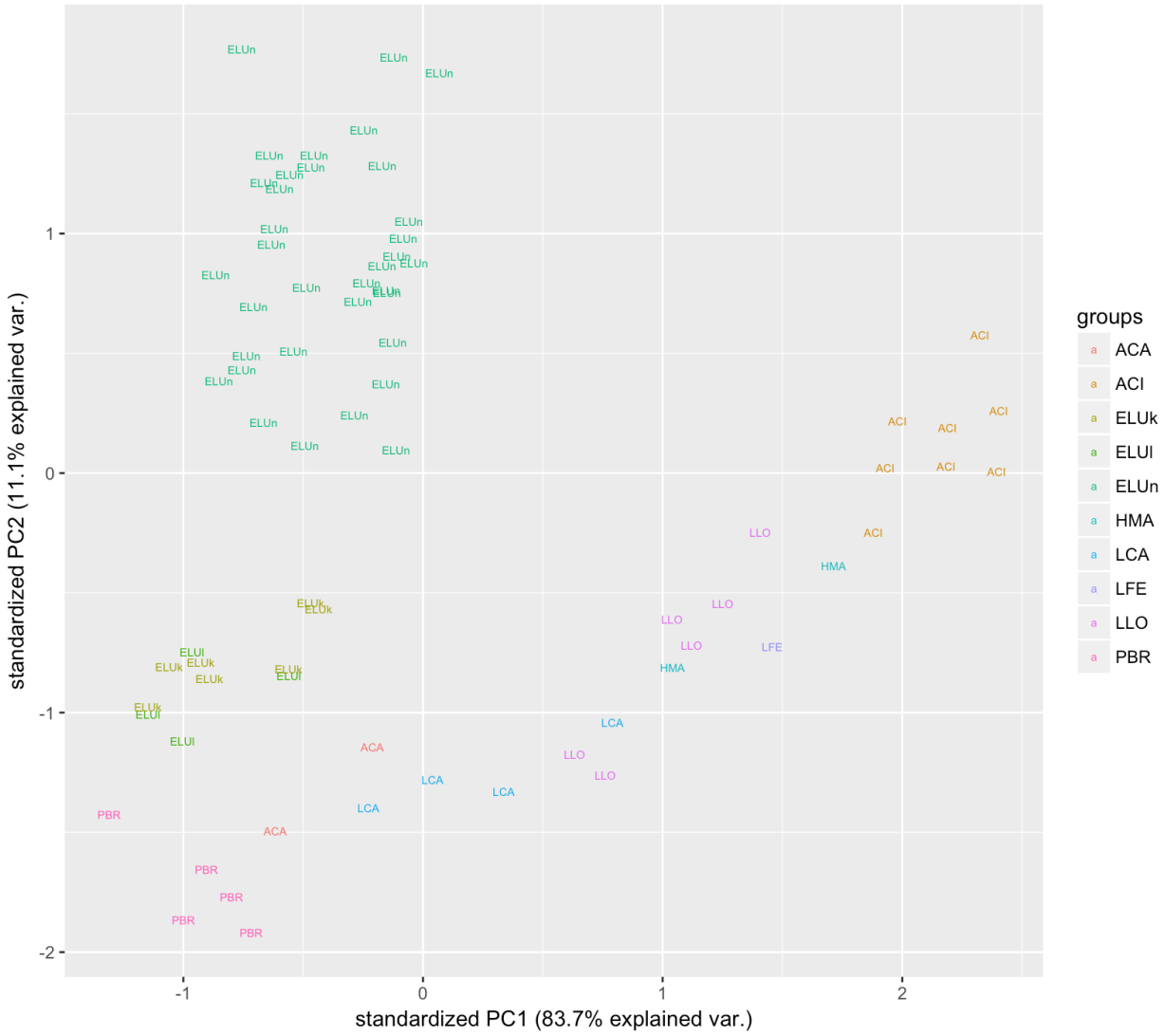

Appendix Figure 4, Plot of the first two principal components of the three forelimb across all sampled members of Lutrinae: *Enhydra spp*. is most separated from all other otters by UCP, with *E. l. nereis* separating most.

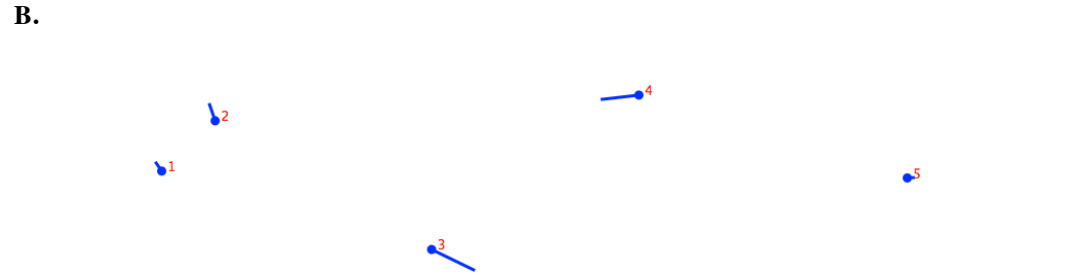

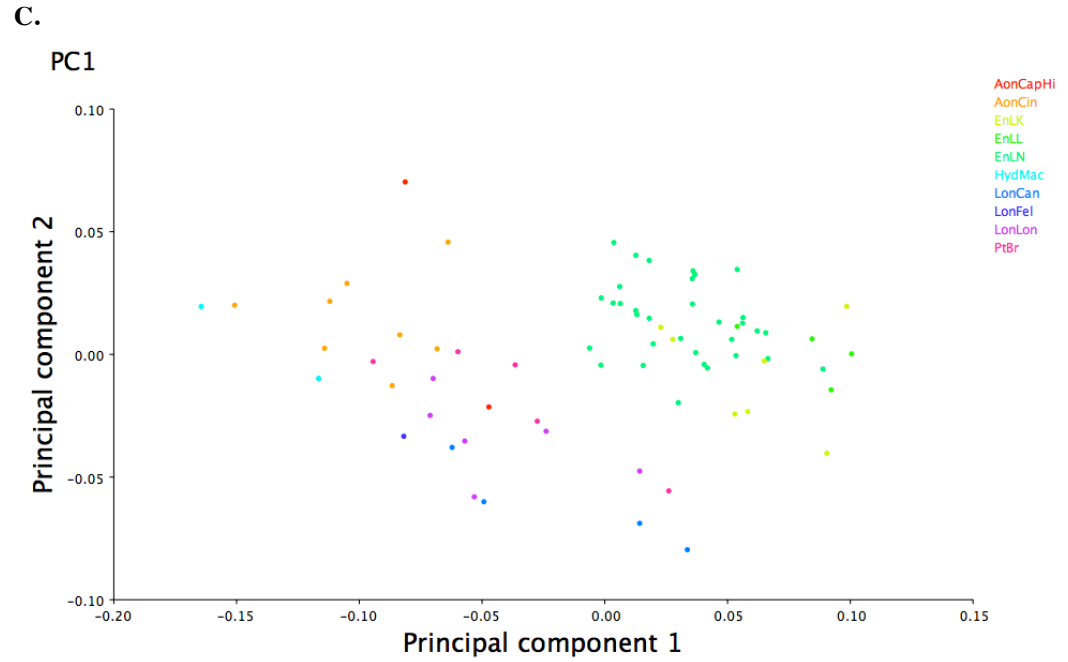

Appendix Figure 6A-C: A. Numbered landmarks of the humerus. B. Lollipop graph displaying landmarks with most variation and in which direction. C. Plot of the first two principal components of the geometric morphometrics analysis of the humerus across all sampled members of Lutrinae.

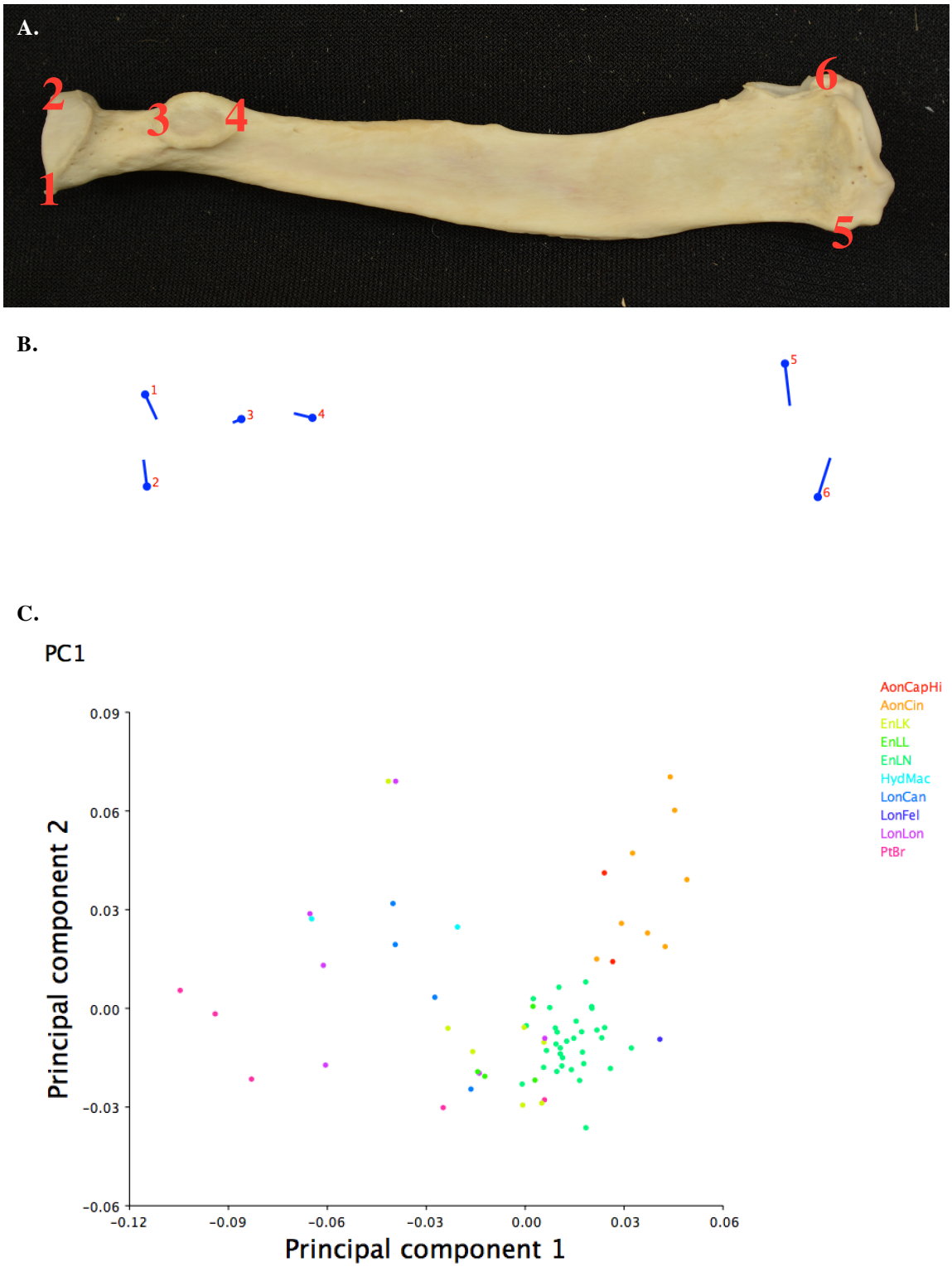

Appendix Figure 7A-C: A. Numbered landmarks of the radius. B. Lollipop graph displaying landmarks with most variation and in which direction. C. Plot of the first two principal components of the geometric morphometrics analysis of the radius across all sampled members of Lutrinae.

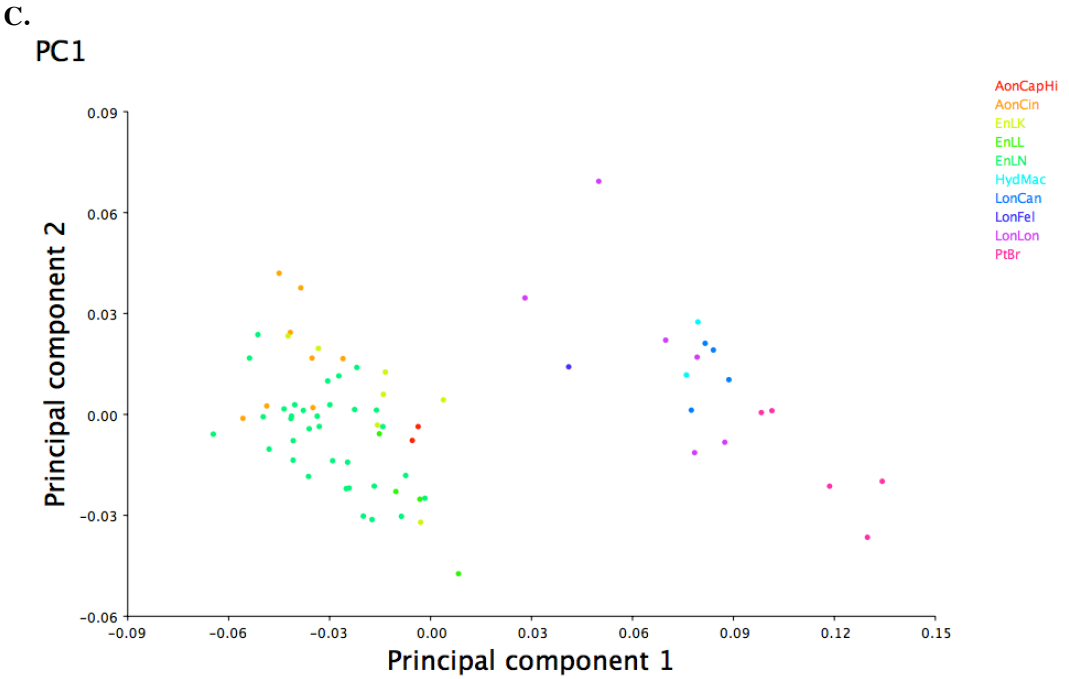

Appendix Figure 8A-C: A. Numbered landmarks of the ulna. B. Lollipop graph displaying landmarks with most variation and in which direction. C. Plot of the first two principal components of the geometric morphometrics analysis of the ulna across all sampled members of Lutrinae.

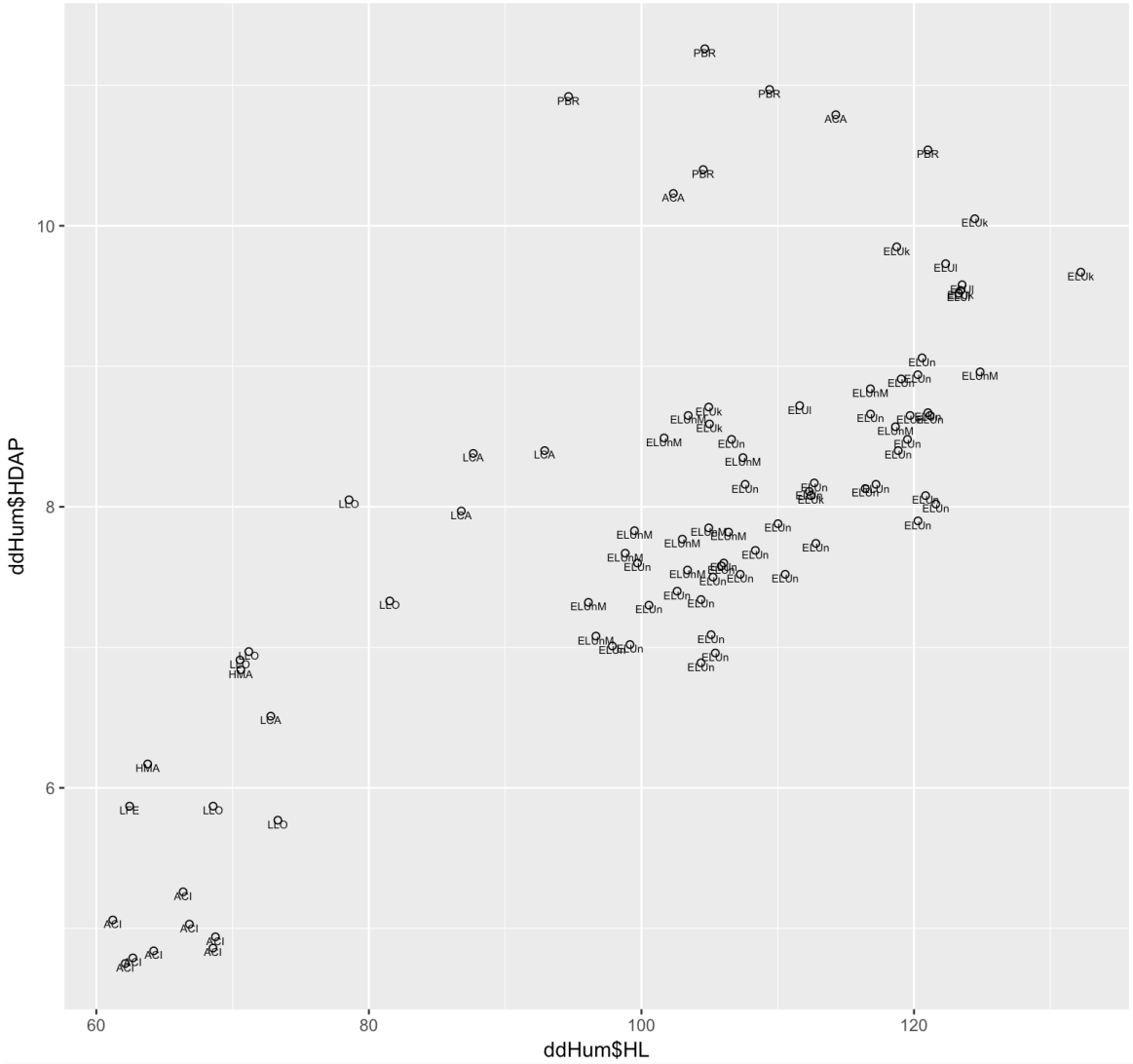

Appendix Figure 9, HDAP/HL**:** California sea otters plot almost exclusively below all other otters and have relatively small HDAPs for their HLs when compared to other sea otter specimens. *Pteronura* and *A. capensis* have very large HDAP/HL ratios.

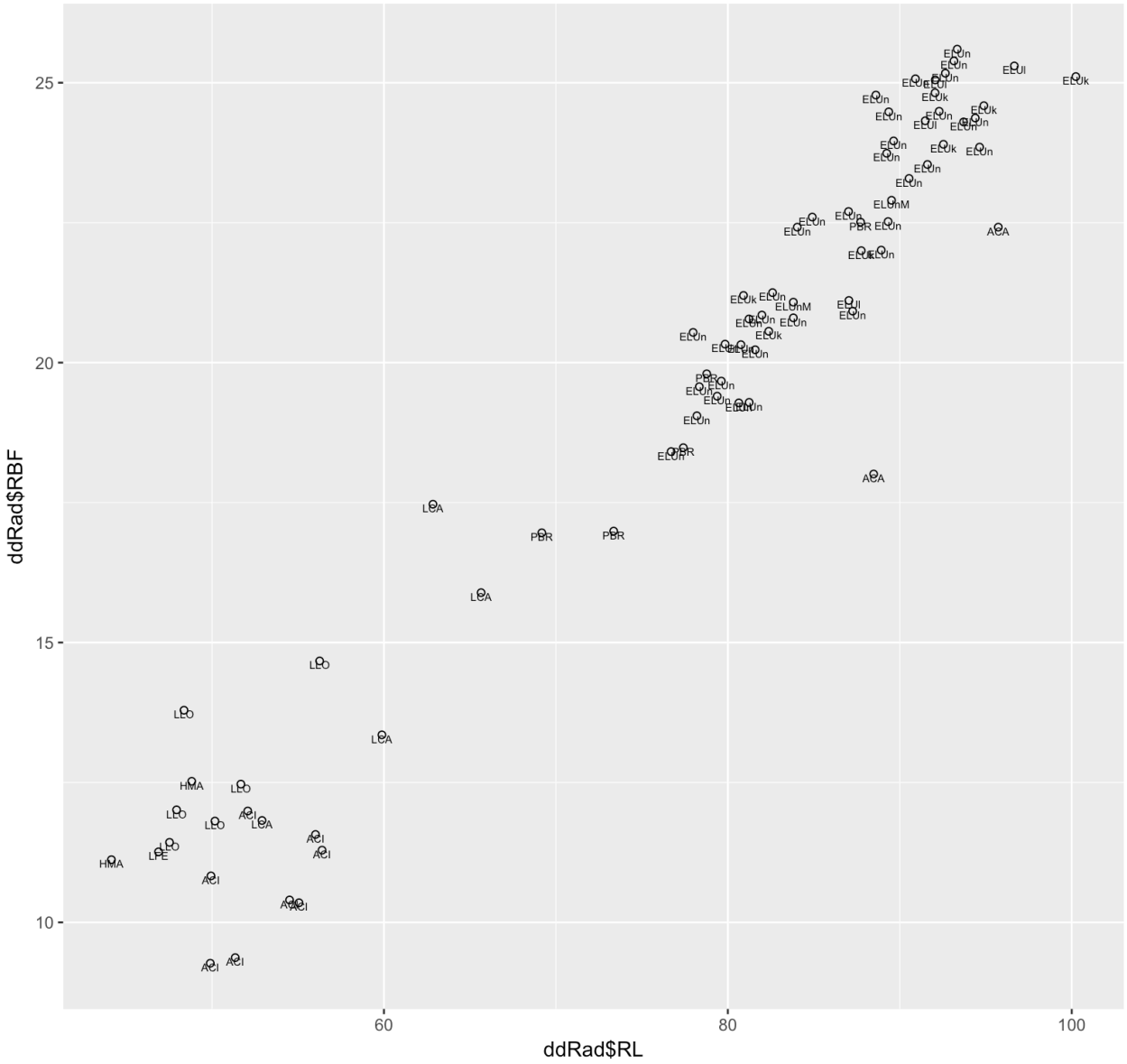

Appendix Figure 10, RBF/RL: *Enhydra*, while somewhat intragenerically indistinct, has some trends. California sea otters tend to have smaller RL measurements overall. Midden specimens tend to be larger than modern California sea otters. Some modern specimens, however, have exceedingly large radial lengths and RBFs for their size (top right corner). *Pteronura*, for its overall body size, has a notably small RL and RBF.

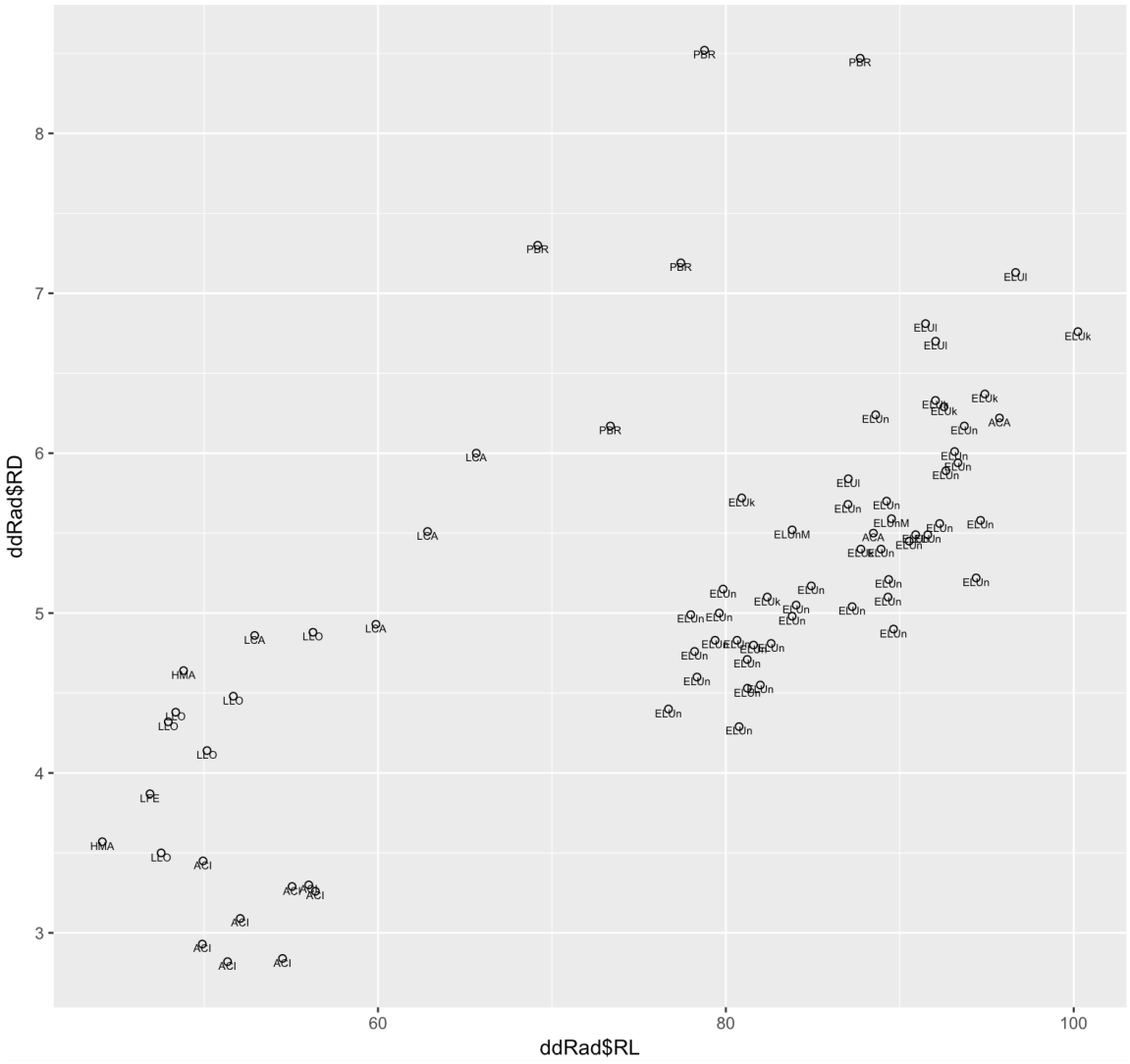

Appendix Figure 11, RD/RL**:** California sea otters very clearly have smaller radial diameters (RD) relative to their RL than other sea otter subspecies. The sea otter specimens with the largest RDs are *E. lutris kenyoni* and *E. lutris lutris*. *A. capensis* also plots among these specimens. Although similar in overall body size, *Pteronura* has a vastly larger RD. More generally, there is some divide among more aquatic and more terrestrial otter species.

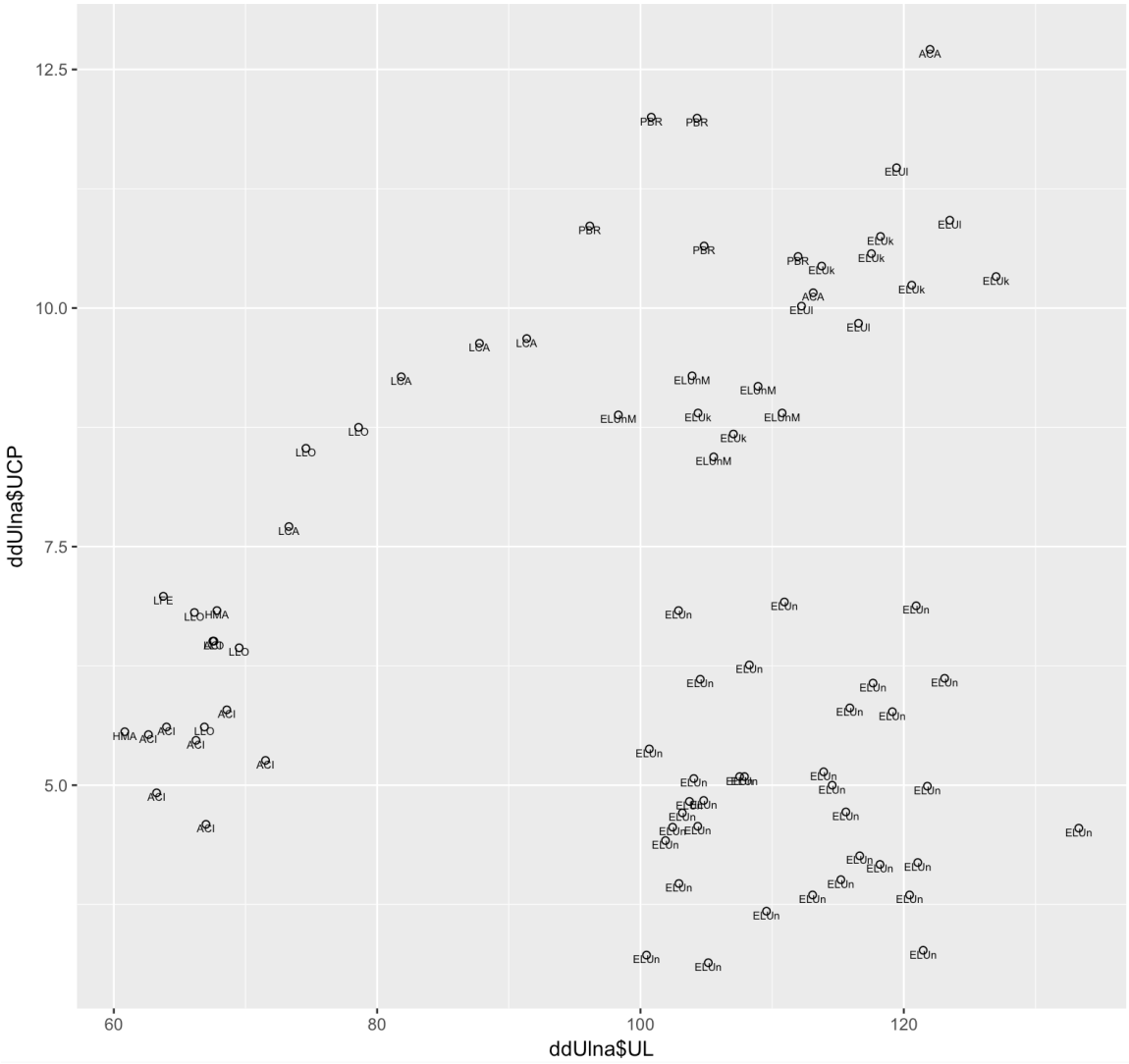

Appendix Figure 12, UCP/UL**:** As previously noted, California sea otters have much smaller UCP measurements for their ULs. Midden specimens plot together and among two Alaskan specimens, as opposed to with modern California sea otters.

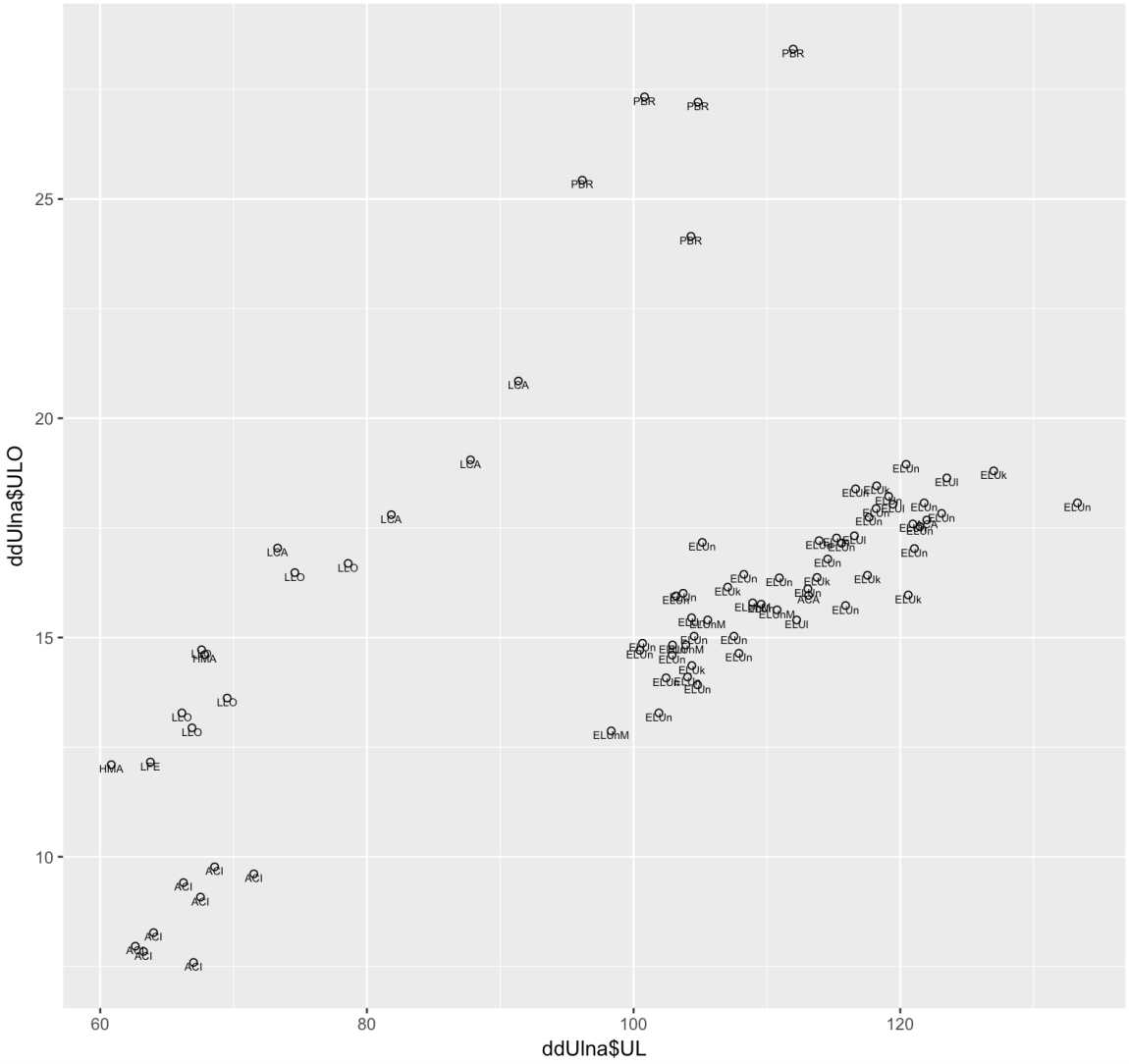

Appendix Figure 13, ULO/UL**:** *Enhydra* and *Aonyx* are characterized by having relatively small ULO measurements for their size. *Aonyx capensis* plots well within the *Enhydra* grouping. All other otters have have concomitantly increasing ULO length for their UL.

TABLES, CODE, & DATA OUTPUT:

Raw measurements and photos available upon request. Please contact author at brandonhupka@g.ucla.edu.

TABLE 1, SPECIES COUNT:		
Enhydra lutris spp.		*Lontra felina* 1
……..*lutris* 4		*Lontra longicaudis spp.*
……..*kenyoni* 7		……..*annectens* 1
……..*nereis* 36		……..*enudris* 2
Aonyx capensis spp.		……..*longicaudis* 3
……..*hindei* 2		*Pteronura brasiliensis* 5
Aonyx cinereus 9		Midden specimens:
Hydrictis maculicollis 2		*Enhydra lutris nereis*
Lontra canadensis spp.		……..*humerus* 14
……..*lataxina* 1		……..*radius* 2
……..*mira* 1		……..*ulna* 5
……..*sonora* 1		
……..*vaga* 1		

TABLE 2, LINEAR MEASUREMENT ABBREVIATIONS:	
HUMERUS:	
HL	greatest length of humerus
HD	smallest transverse diameter of humeral diaphysis
HPAP	anteroposterior depth of proximal humerus
HEB	humerus epicondylar mediolateral breadth
HDAP	humerus anteoposterior compression of the distal articular surface at the trochlear notch
HDAB	humeral distal articulation breadth from the trochlea to the capitulum
RADIUS:	

TABLE 2, LINEAR MEASUREMENT ABBREVIATIONS:	
RL	greatest length of the radius
RD	smallest diameter of the diaphysis of the radius
RPML	mediolateral breadth of the proximal radius
RPAP	anteroposterior depth of the proximal radius
RDML	mediolateral breadth of the distal radius
RDAP	anteroposterior depth of the distal radius
RMLA	mediolateral breadth of the distal articulation of the radius
RAPA	anteroposterior depth of the distal articulation of the radius
RBF	distance from distal side of bicipital tuberosity of radius to proximal radial articular surface
ULNA:	
UL	greatest length of the ulna
ULO	length of the olecranon process of the ulna
UOD	anteroposterior depth of the olecranon process
UPA	anteroposterior depth across the processus anconeus of the ulna
UCP	mediolateral breadth across the coronoid process and radial notch

TABLE 3, FUNCTIONAL RATIOS & INDICES:	
RBF/RL	mechanical advantage of biceps brachii
RD/RL	radial robusticity index
HDAP/HL	trochlear notch robusticity index
UCP/UL	antebrachial rotational index
ULO/UL	olecranon index

LINEAR MEASUREMENT PCA LOADINGS:	PC1:	PC2:
HUMERUS:		
HL	-0.3535878	0.17882864
HD	-0.4790850	0.44234234

LINEAR MEASUREMENT PCA LOADINGS:	PC1:	PC2:
HPAP	-0.4357944	0.04459247
HEB	-0.4083961	-0.18058055
HDAP	-0.3023737	-0.85474259
HDAB	-0.4442063	0.08468084
RADIUS:		
RL	-0.2835148	0.58078116
RD	-0.2843233	-0.46670423
RPML	-0.3009074	-0.12527835
RPAP	-0.3335614	-0.04533657
RDML	-0.3410436	-0.08049499
RDAP	-0.3725047	-0.16170174
RMLA	-0.3590154	-0.01179165
RAPA	-0.3398471	-0.28097573
RBF	-0.3708267	0.56162001
ULNA:		
UL	-0.3447441	0.3077080
ULO	-0.4564364	0.1018582
UOD	-0.5059665	0.1874281
UPA	-0.5111201	0.2124733
UCP	-0.3944255	-0.9025888
BRACHIUM & ANTEBRACHIUM WITH HL, RL, UL:		
HL	-0.19562610	0.111798710
HD	-0.26161594	0.135230484

LINEAR MEASUREMENT PCA LOADINGS:	PC1:	PC2:
HPAP	-0.24378980	0.078408042
HEB	-0.23335647	0.022286531
HDAP	-0.17782056	-0.149776025
HDAB	-0.24847107	0.089329737
RL	-0.19406175	0.167912290
RD	-0.19927244	-0.169256683
RPML	-0.20949659	-0.007018740
RPAP	-0.23102200	-0.014872303
RDML	-0.23667618	0.002095036
RDAP	-0.25896457	-0.010695818
RMLA	-0.24727137	0.012469784
RAPA	-0.23640174	-0.053055326
RBF	-0.25525625	0.197716988
UL	-0.19344977	0.135351212
ULO	-0.20427741	-0.183854114
UOD	-0.24408525	-0.061867040
UPA	-0.24758917	-0.058758519
UCP	-0.07821984	-0.879465886
BRACHIUM & ANTEBRACHIUM WITHOUT HL, RL, UL:		
HD	-0.27505958	0.163486535
HPAP	-0.25680131	0.102584011
HEB	-0.24739934	0.049530614
HDAP	-0.19084993	-0.133983855
HDAB	-0.26186167	0.115939253
RD	-0.21427799	-0.149390712
RPML	-0.22263061	0.017746475

LINEAR MEASUREMENT PCA LOADINGS:	**PC1:**	**PC2:**
RPAP	-0.24483739	0.006798095
RDML	-0.25086366	0.026913984
RDAP	-0.27517999	0.019396377
RMLA	-0.26174568	0.036915002
RAPA	-0.25230526	-0.023712074
RBF	-0.26600449	0.218161580
ULO	-0.22186629	-0.149060994
UOD	-0.25997585	-0.036001937
UPA	-0.26388259	-0.030709299
UCP	-0.09348268	-0.911671352
Enhydra ONLY BRACHIUM & ANTEBRACHIUM WITHOUT HL, RL, UL:		
HD	-0.1343905	0.1951153
HPAP	-0.1207864	0.1473104
HEB	-0.1359578	0.2010623
HDAP	-0.1845895	0.1597657
HDAB	-0.1424088	0.1794616
RD	-0.2322335	0.1994361
RPML	-0.1187462	0.1795475
RPAP	-0.2001143	0.1879579
RDML	-0.1150566	0.1461008
RDAP	-0.1359262	0.1134239
RMLA	-0.1681885	0.1137439
RAPA	-0.1444374	0.1169143
RBF	-0.1404345	0.2704351
ULO	-0.1014773	0.2767097
UOD	-0.2150801	0.2006678

LINEAR MEASUREMENT PCA LOADINGS:	PC1:	PC2:
UPA	-0.2038150	0.3187030
UCP	-0.7666486	-0.6183625

R CODE:

```
setwd("/Users/BHupka/Desktop/OTTER FILES/R FILES")
ddAnt <- read.csv("AntebBrach.csv")
ddAntMinus <- read.csv("AntebBrachMinusHLRLUL.csv")
ddEnMinus <- read.csv("EnhydraAntebBrachMinus.csv")
ddHum <- read.csv("Humerus.csv")
ddRad <- read.csv(“Radius.csv")
ddUlna <- read.csv("Ulna.csv")

install.packages("curl")
install.packages(c('devtools','curl'))
install.packages("ggplot2")
install.packages('Rcpp', dependencies = TRUE)
library(devtools)
install_github("ggbiplot", "vqv", force=T)
library(ggbiplot)
library(ggplot2)

#BRACHIUM & ANTEBRACHIUM
logdd <- log(ddAnt[,3:22])
antebbrachPCA <-prcomp(logdd)
antebbrachPCA
logAnt <- ggbiplot(antebbrachPCA, obs.cale=1, var.scale=1, groups=ddAnt$Abbr, ellipse=F,
circle=F, var.axes = FALSE, labels=ddAnt$Abbr, labels.size = 2)
print(logAnt)
plot(antebbrachPCA, type="l")

#ENHYDRA BRACHIUM & ANTEBRACHIUM MINUS HL, RL, UL
specName <- ddEnMinus$Abbr
logEnAb <- log(ddEnMinus[,3:19])
enhydrabrachPCA <- prcomp(logEnAb)
enhydrabrachPCA
logEnhydra <- ggbiplot(enhydrabrachPCA, obs.cale=1, var.scale=1, groups=specName,
ellipse=F, circle=F, var.axes = FALSE, labels=specName, labels.size = 2)
print(logEnhydra)
plot(enhydrabrachPCA, type="l")

#Body size by PC1 minus HL, RL, UL for all Lutrinae
```

```
specName <- ddAnt$Abbr
logAB <- log(ddAntMinus[,3:19])
logABMinus <- prcomp(logAB)
logABMinus
pc1AB <- logABMinus$x[,1]
bsizeAB <- ggplot(ddAntMinus, aes(x = log(ddAntMinus$GEOMEAN), y = pc1AB, label =
specName)) + geom_point(shape = 1) +
  geom_text(aes(label = specName), hjust = 0.5, vjust = 1, size = 2) + geom_smooth(method =
lm, se = FALSE)
bsizeAB

#Body size by PC1 minus HL, RL, UL for Enhydra
specNameEn <- ddEnMinus$Abbr
logEnAB <- log(ddEnMinus[,3:19])
logEnABMinus <- prcomp(logEnAB)
logEnABMinus
pc1EnAB <- logEnABMinus$x[,1]
bsizeEnAB <- ggplot(ddEnMinus, aes(x = log(ddEnMinus$GEOMEAN), y = pc1EnAB, label =
specNameEn)) + geom_point(shape = 1) +
  geom_text(aes(label = specNameEn), hjust = 0.5, vjust = 1, size = 2) + geom_smooth(method =
lm, se = FALSE)
bsizeEnAB

#HUMERUS
ddcat <-ddHum[,2]
logHum <- log(ddHum[,3:8])
logHum.pca <- prcomp(logHum)
plot(logHum.pca, type="l")
logHum.pca
logHum <- ggbiplot(logHum.pca, obs.scale=1, var.scale=1, groups=ddHum$Abbr, ellipse=F,
circle=F, var.axes = FALSE, labels=ddHum$Abbr, labels.size = 2)
print(logHum)

#RADIUS
logRad <- log(ddRad[,3:11])
logRad.pca <- prcomp(logRad)
plot(logRad.pca, type="l")
logRad.pca
gRad <- ggbiplot(logRad.pca, obs.scale=1, var.scale=1, groups=ddRad$Abbr, ellipse=F,
circle=F, var.axes = FALSE, labels=ddRad$Abbr, labels.size = 2)
print(gRad)

#ULNA
logUlna <- log(ddUlna[,3:7])
logUlna.pca <- prcomp(logUlna)
plot(logUlna.pca, type="l")
```

```
logUlna.pca
plotlogUlna <- ggbiplot(logUlna.pca, obs.scale=1, var.scale=1, groups=ddUlna$Abbr, ellipse=F,
circle=F, var.axes = FALSE, labels=ddUlna$Abbr, labels.size = 2)
plot(plotlogUlna)

#RATIO GRAPHS
radNam <- ddRad$Abbr
rbfRL <- ggplot(ddRad, aes(x = ddRad$RL, y = ddRad$RBF, label = radNam)) +
geom_point(shape = 1) +
  geom_text(aes(label = radNam), hjust = 0.5, vjust = 1, size = 2)
rbfRL

rdRL <- ggplot(ddRad, aes(x = ddRad$RL, y = ddRad$RD, label = radNam)) +
geom_point(shape = 1) +
  geom_text(aes(label = radNam), hjust = 0.5, vjust = 1, size = 2)
rdRL

humNam <- ddHum$Abbr
hdHL <- ggplot(ddHum, aes(x = ddHum$HL, y = ddHum$HD, label = humNam)) +
geom_point(shape = 1) +
  geom_text(aes(label = humNam), hjust = 0.5, vjust = 1, size = 2)
hdHL

hdapHL <- ggplot(ddHum, aes(x = ddHum$HL, y = ddHum$HDAP, label = humNam)) +
geom_point(shape = 1) +
  geom_text(aes(label = humNam), hjust = 0.5, vjust = 1, size = 2)
hdapHL

ulnNam <- ddUlna$Abbr
ucpUL <- ggplot(ddUlna, aes(x = ddUlna$UL, y = ddUlna$UCP, label = ulnNam)) +
geom_point(shape = 1) +
  geom_text(aes(label = ulnNam), hjust = 0.5, vjust = 1, size = 2)
ucpUL

uloUL <- ggplot(ddUlna, aes(x = ddUlna$UL, y = ddUlna$ULO, label = ulnNam)) +
geom_point(shape = 1) +
  geom_text(aes(label = ulnNam), hjust = 0.5, vjust = 1, size = 2)
uloUL

upaUL <- ggplot(ddUlna, aes(x = ddUlna$UL, y = ddUlna$UPA, label = ulnNam)) +
geom_point(shape = 1) +
  geom_text(aes(label = ulnNam), hjust = 0.5, vjust = 1, size = 2)
upaUL
```

MORPHOJ OUTPUT:
HUMERUS:

New Procrustes fit:
Dataset 'newDataset'

5 landmarks in 2 dimensions.
The dataset contains 72 observations, of which 72 are included for analyses.

Average shape:

Lmk.	Axis 1 (x)	Axis 2 (y)
1	-0.49185514	-0.01301219
2	-0.40682467	0.06668545
3	-0.06255897	-0.13725286
4	0.26719679	0.10745107
5	0.69404198	-0.02387147

Procrustes sums of squares: 0.42576122861713106
Tangent sums of squares: 0.4212123088480486

Data matrices in this dataset:
- newDataset, raw data
- newDataset, centroid size
- newDataset, Procrustes coordinates

New Procrustes fit:
Dataset 'newDataset'

5 landmarks in 2 dimensions.
The dataset contains 72 observations, of which 72 are included for analyses.

Average shape:

Lmk.	Axis 1 (x)	Axis 2 (y)
1	-0.49185514	-0.01301219
2	-0.40682467	0.06668545
3	-0.06255897	-0.13725286
4	0.26719679	0.10745107
5	0.69404198	-0.02387147

Procrustes sums of squares: 0.42576122861713106
Tangent sums of squares: 0.4212123088480486

Data matrices in this dataset:
- newDataset, raw data
- newDataset, centroid size
- newDataset, Procrustes coordinates

Principal Component Analysis: PCA: CovMatrix, newDataset, Procrustes coordinates

	Eigenvalues	% Variance	Cumulative %
1.	0.00405320	68.321	68.321
2.	0.00081078	13.667	81.988
3.	0.00040199	6.776	88.764
4.	0.00031094	5.241	94.005
5.	0.00023197	3.910	97.915
6.	0.00012369	2.085	100.000

Total variance: 0.00593257

Variance of the eigenvalues: 0.0000019245506
Eigenvalue variance scaled by total variance: 0.05468
Eigenvalue variance scaled by total variance and number of variables: 0.39371
Note: hroughout all calculations of eigenvalue variances, the dimensionality used was 6.
Please double-check because this dimensionality may not be appropriate for all situations.

Principal Component Coefficients

	PC1	PC2	PC3	PC4	PC5	PC6
x1	-0.088024	0.325819	-0.140756	-0.093039	0.022227	-0.644237
y1	0.127973	-0.006599	0.153145	0.573171	-0.408247	-0.151143
x2	-0.088943	-0.040697	-0.219925	-0.075586	-0.365997	0.657606
y2	0.255875	-0.048453	-0.539904	-0.290156	0.428252	0.056045
x3	0.666141	-0.309984	0.413854	0.040246	0.252706	0.025675
y3	-0.321856	0.350538	0.597589	-0.207534	0.308938	0.234849
x4	-0.584427	-0.481116	-0.021746	0.230827	0.290226	-0.077763
y4	-0.067105	-0.412019	0.074581	-0.518156	-0.462955	-0.233283
x5	0.095253	0.505979	-0.031427	-0.102449	-0.199161	0.038718
y5	0.005114	0.116534	-0.285412	0.442676	0.134013	0.093533

RADIUS:

New Procrustes fit:
Dataset 'newDataset'

6 landmarks in 2 dimensions.
The dataset contains 71 observations, of which 71 are included for analyses.

Average shape:

Lmk.	Axis 1 (x)	Axis 2 (y)
1	-0.37269784	0.04993859
2	-0.37018599	-0.08037166
3	-0.23630767	0.01512689
4	-0.13561261	0.01687407
5	0.53411515	0.09376669
6	0.58068896	-0.09533457

Procrustes sums of squares: 0.16751682825693487
Tangent sums of squares: 0.16659073261832363

Data matrices in this dataset:
- newDataset, raw data
- newDataset, centroid size
- newDataset, Procrustes coordinates

Principal Component Analysis: PCA: CovMatrix, newDataset, Procrustes coordinates

	Eigenvalues	% Variance	Cumulative %
1.	0.00107579	45.204	45.204
2.	0.00060467	25.408	70.611
3.	0.00032124	13.498	84.110
4.	0.00012746	5.356	89.465
5.	0.00009641	4.051	93.517
6.	0.00006522	2.741	96.257
7.	0.00005699	2.395	98.652
8.	0.00003208	1.348	100.000

Total variance: 0.00237987

Variance of the eigenvalues: 0.0000001190308
Eigenvalue variance scaled by total variance: 0.02102
Eigenvalue variance scaled by total variance and number of variables: 0.19215
Note: throughout all calculations of eigenvalue variances, the dimensionality used was 8.
Please double-check because this dimensionality may not be appropriate for all situations.

Principal Component Coefficients

	PC1	PC2	PC3	PC4	PC5	PC6	PC7	PC8
x1	0.155726	0.131683	0.184612	0.362951	-0.665236	-0.052777	-0.094376	-0.174065
y1	-0.334489	0.342426	-0.107343	0.311613	0.024733	-0.204994	0.529618	0.176190
x2	-0.044852	0.263705	0.537555	-0.139739	0.548811	-0.051186	0.013012	0.076214
y2	0.360640	0.158610	-0.246233	0.193729	0.268004	0.225944	-0.555326	0.072062
x3	-0.104595	-0.257748	-0.336553	-0.194230	-0.082381	0.540626	0.222497	0.447580
y3	-0.043082	-0.339038	0.267930	-0.185208	0.008421	0.354679	0.215392	-0.618151
x4	-0.243257	-0.271592	-0.503473	-0.034851	0.210398	-0.483885	-0.135746	-0.360811
y4	0.059172	-0.365010	0.264869	-0.373851	-0.240070	-0.448063	-0.168528	0.425685
x5	0.066844	0.486918	-0.080650	-0.489800	-0.183537	0.032449	-0.057721	-0.115002
y5	-0.578802	0.106513	0.041031	0.110715	-0.101092	0.185630	-0.366261	0.011777
x6	0.170134	-0.352967	0.198508	0.495670	0.171945	0.014773	0.052334	0.126084
y6	0.536560	0.096499	-0.220254	-0.056997	0.040004	-0.113196	0.345104	-0.067564

ULNA:

New Procrustes fit:
Dataset 'newDataset'

5 landmarks in 2 dimensions.
The dataset contains 72 observations, of which 72 are included for analyses.

Average shape:

Lmk.	Axis 1 (x)	Axis 2 (y)
1	-0.31060718	-0.02109720
2	-0.34168351	0.08656155
3	-0.17432364	-0.04403129
4	-0.03568138	-0.03767318
5	0.86229572	0.01624012

Procrustes sums of squares: 0.25839421991445854
Tangent sums of squares: 0.2563268280209871

Data matrices in this dataset:
- newDataset, raw data
- newDataset, centroid size
- newDataset, Procrustes coordinates

Principal Component Analysis: PCA: CovMatrix, newDataset, Procrustes coordinates

	Eigenvalues	% Variance	Cumulative %
1.	0.00274943	76.157	76.157
2.	0.00040616	11.250	87.407
3.	0.00021718	6.016	93.423
4.	0.00012079	3.346	96.768
5.	0.00006432	1.782	98.550
6.	0.00005235	1.450	100.000

Total variance: 0.00361024

Variance of the eigenvalues: 0.0000009367820
Eigenvalue variance scaled by total variance: 0.07187
Eigenvalue variance scaled by total variance and number of variables: 0.51749
Note: throughout all calculations of eigenvalue variances, the dimensionality used was 6.
Please double-check because this dimensionality may not be appropriate for all situations.

Principal Component Coefficients

	PC1	PC2	PC3	PC4	PC5	PC6
x1	-0.153314	0.160296	0.206986	0.314329	0.612623	-0.370034
y1	-0.042272	-0.381990	-0.678428	-0.021620	0.178220	-0.250760
x2	-0.353132	-0.450337	0.109696	0.224952	-0.487596	0.218785
y2	0.525867	-0.268974	0.560586	0.084423	0.054952	0.049729
x3	0.133774	-0.036867	0.017075	-0.849590	0.121707	0.107290
y3	-0.304207	0.433667	-0.047411	0.044068	0.191037	0.668116
x4	0.596615	0.377416	-0.371947	0.283968	-0.274541	0.067528
y4	-0.232599	0.421066	0.168082	-0.180345	-0.471652	-0.531674
x5	-0.223943	-0.050508	0.038189	0.026340	0.027807	-0.023569
y5	0.053211	-0.203769	-0.002829	0.073474	0.047443	0.064590

REFERENCES:

Andersson, Ki. "Elbow-joint Morphology As a Guide to Forearm Function and Foraging Behaviour in Mammalian Carnivores." Zoological Journal of the Linnean Society. 142.1 (2004): 91-104. Print.

Arzi, B, JN Winer, PH Kass, and FJ Verstraete. "Osteoarthritis of the Temporomandibular Joint in Southern Sea Otters (*Enhydra lutris nereis*)." Journal of Comparative Pathology. 149.4 (2013): 486-94. Print.

Botton-Divet, Léo, Raphaël Cornette, Anne-Claire Fabre, Anthony Herrel, and Alexandra Houssaye. "Morphological Analysis of Long Bones in Semi-Aquatic Mustelids and Their Terrestrial Relatives." Integrative and Comparative Biology. 56.6 (2016): 1298-1309. Print.

Botton-Divet, Léo, Alexandra Houssaye, Anthony Herrel, Anne-Claire Fabre, and Raphaël Cornette. "Swimmers, Diggers, Climbers and More, a Study of Integration Across the Mustelids' Locomotor Apparatus (Carnivora: Mustelidae)." Evolutionary Biology : Evolutionary Biology. 45.2 (2018): 182-195. Print.

Braje, T. J. (2007). *Archaeology, human impacts, and historical ecology on san miguel island, california* (Order No. 3276036). Available from ProQuest Dissertations & Theses A&I; ProQuest Dissertations & Theses Global. (304832009). Retrieved from https://search.proquest.com/docview/304832009?accountid=14512

Carter, S.K, and F.C.W Rosas. "Biology and Conservation of the Giant Otter Pteronura Brasiliensis." Mammal Review. 27.1 (1997): 1-26. Print.

Cronin, M A, J Bodkin, B Ballachey, J Estes, and J C. Patton. "Mitochondrial-dna Variation Among Subspecies and Populations of Sea Otters (*Enhydra lutris*)." *Journal of Mammalogy*. 77.2 (1996): 546-557. Print.

Doroff, A. & Burdin, A. 2015. *Enhydra lutris*. The IUCN Red List of Threatened Species 2015: e.T7750A21939518. http://dx.doi.org/10.2305/IUCN.UK.2015-2.RLTS.T7750A21939518.en. Downloaded on 06 June 2018.

Estes, James A. *Enhydra Lutris*. Washington: Soc, 1980. Print.

Estes, J A, M L. Riedman, M M. Staedler, M T. Tinker, and B E. Lyon. "Individual Variation in Prey Selection by Sea Otters: Patterns, Causes and Implications." Journal of Animal Ecology. 72.1 (2003): 144-155. Print.

Fabre, Anne-Claire, Raphael Cornette, Anjali Goswami, and Stéphane Peigné. "Do Constraints Associated with the Locomotor Habitat Drive the Evolution of Forelimb Shape? A Case Study in Musteloid Carnivorans." *Journal of Anatomy*. 226.6 (2015): 596-610. Print.

Fujii, J.A, K Ralls, and M.T Tinker. "Ecological Drivers of Variation in Tool-Use Frequency Across Sea Otter Populations." Behavioral Ecology. 26.2 (2015): 519-526. Print.

Howard, Lot D. Muscular Anatomy of the Forelimb of the Sea Otter (*Enhydra lutris*). San Francisco: California Academy of Sciences, 1973. Print.

Jackson, JB, MX Kirby, WH Berger, KA Bjorndal, LW Botsford, BJ Bourque, RH Bradbury, R Cooke, J Erlandson, JA Estes, TP Hughes, S Kidwell, CB Lange, HS Lenihan, JM Pandolfi, CH Peterson, RS Steneck, MJ Tegner, and RR Warner. "Historical Overfishing and the Recent Collapse of Coastal Ecosystems." Science (New York, N.Y.). 293.5530 (2001): 629-37. Print.

Kenyon, Karl W. The Sea Otter in the Eastern Pacific Ocean. Washington: U.S. Government printing Office, 1969. Print.

Larivière, Serge. *Lontra Felina*. Washington: Soc, 1998. Print.

Larivière, Serge, and Lyle R. Walton. *Lontra Canadensis*. Washington: Soc, 1998. Print.

Larivière, Serge. *Lontra Longicaudis*. Washington: Soc, 1999. Print.

Larivière, Serge. *Aonyx Capensis*. Washington: Soc, 2001. Print.

Larivière, Serge. *Amblonyx Cinereus*. Mammalian Species. 720 (2003): 1-5. Print.

Meachen-Samuels, Julie, and Valkenburgh B. Van. "Forelimb Indicators of Prey-Size Preference in the Felidae." *Journal of Morphology*. 270.6 (2009): 729-744. Print.

Ross, Stephen. (2002). The effect of a simple feeding enrichment strategy on the behavior of two Asian small-clawed otters (*Aonyx cinerea*). Aquatic Mammals. 28. 113-120.

Steneck, Robert S, Michael H. Graham, Bruce J. Bourque, Debbie Corbett, Jon M. Erlandson, James A. Estes, and Mia J. Tegner. "Kelp Forest Ecosystems: Biodiversity, Stability, Resilience and Future." Environmental Conservation. 29.4 (2002). Print.

Tarasoff, F J, André Bisaillon, Jean Piérard, and Arville P. Whitt. "Locomotory Patterns and External Morphology of the River Otter, Sea Otter, and Harp Seal (Mammalia)." Canadian Journal of Zoology. 50.7 (1972): 915-929. Print.

Timmis, W. H. 1971. Observations on breeding the oriental short-clawed otter *Amblonyx cinerea* at Chester Zoo. International Zoo Yearbook 11:109–111.

Wilson, Don E. Bogan, Michael A. Brownell, Robert L. Burdin, A. M. Maminov, M. K. 1991. Geographic Variation in Sea Otters, *Enhydra lutris*. http://www.jstor.org/stable/1381977?origin=pubexport.